Supporting Information

Regulate Protonation Path for Enhanced Photocatalytic CO_2 Methanation by Coupled Pt Sites on $WO_{2.9}/TiO_2$

Jiajun Du,[a] Jun Deng,[a] ChangAn Zhou,[a] Hairong Yue,[a] Chong Liu,[a] Patrik Schmuki,[b] Štěpán Kment,[c] Xuemei Zhou[a]*

[a.] School of Chemical Engineering, Sichuan University, No. 24 South Section 1, Yihuan Road, Chengdu, 610065 (P.R.C.). *Email: xuemeizhou@scu.edu.cn;

[b.] Friedrich-Alexander-University Erlangen-Nurnberg Department of Materials Science and Engineering, Martensstraße 7, 91058 Erlangen, Germany;

[c.] Regional Centre of Advanced Technologies and Materials, Czech Advanced Technology and Research Institute, Palacký University, Křížkovského 511/8, 779 00 Olomouc, Czech Republic.

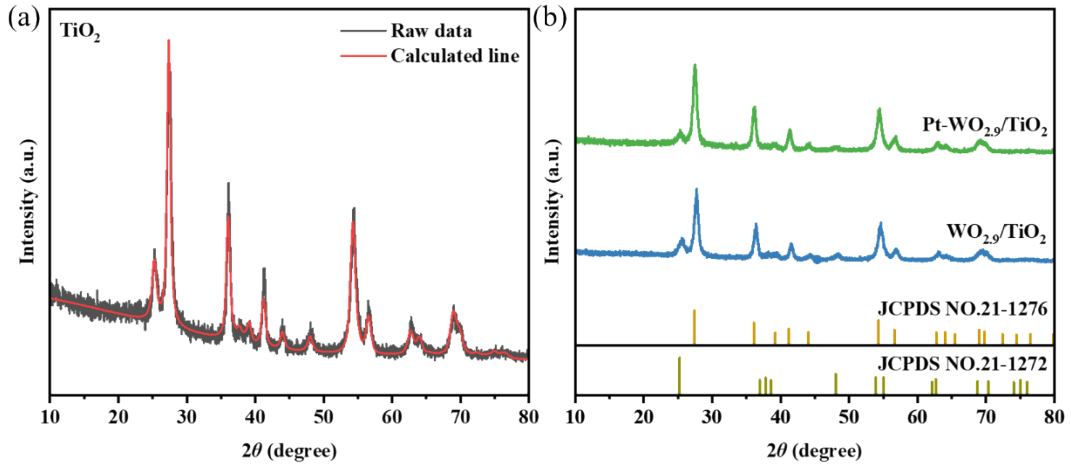

Figure S1. (a) XRD spectrum and Rietveld refinement line of TiO_2 microspheres. (b) XRD spectra of $WO_{2.9}/TiO_2$ and Pt-$WO_{2.9}/TiO_2$.

Table S1. Crystallite size and rutile ratio of different samples

Samples	Anatase		Rutile		Rutile ratio (%)
	2θ (degree)	Crystallite size (nm)	2θ (degree)	Crystallite size (nm)	
TiO_2	25.3	10.2	27.5	11.3	75.1
$WO_{2.9}$-TiO_2	25.3	9.8	27.5	12.0	75.4
Pt-$WO_{2.9}/TiO_2$	25.3	10.5	27.5	11.3	76.5

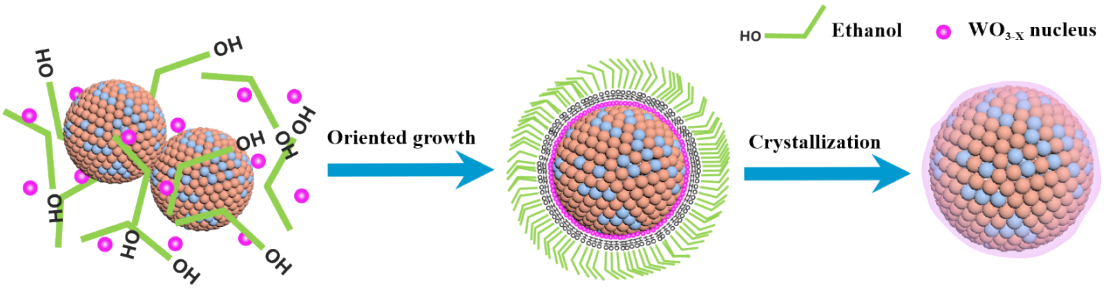

Figure S2. Illustration on the formation scheme of $WO_{2.9}$ film on TiO_2 microspheres.

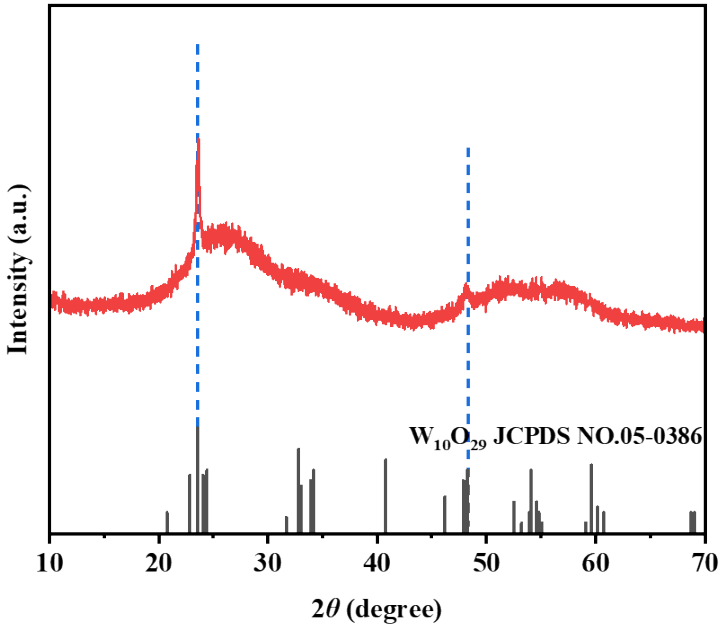

Figure S3. XRD spectrum of $WO_{2.9}$ powders.

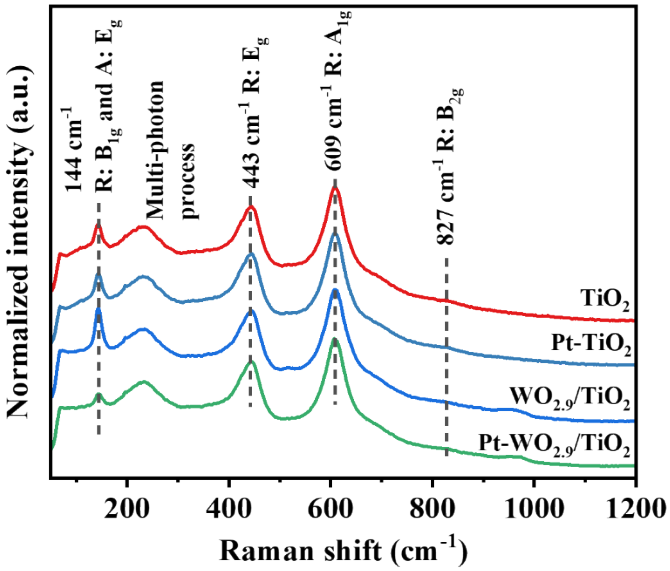

Figure S4. Raman spectra of TiO_2, Pt-TiO_2/$WO_{2.9}$/TiO_2, Pt-$WO_{2.9}$/TiO_2 microspheres.

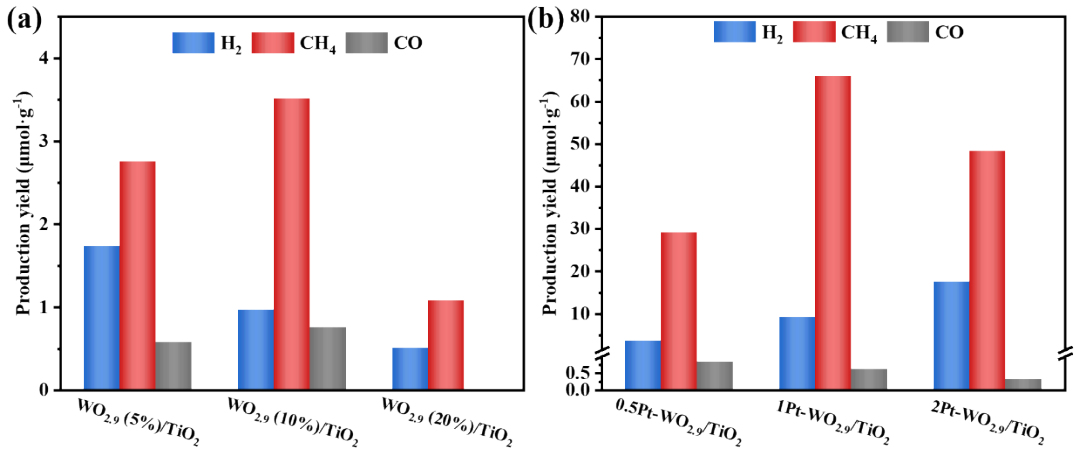

Figure S5. Production yield during photocatalytic CO_2 reduction using (a) $WO_{2.9}$/TiO_2 with different mass ratio of $WO_{2.9}$ and (b) Pt-$WO_{2.9}$/TiO_2 with different mass ratio of Pt.

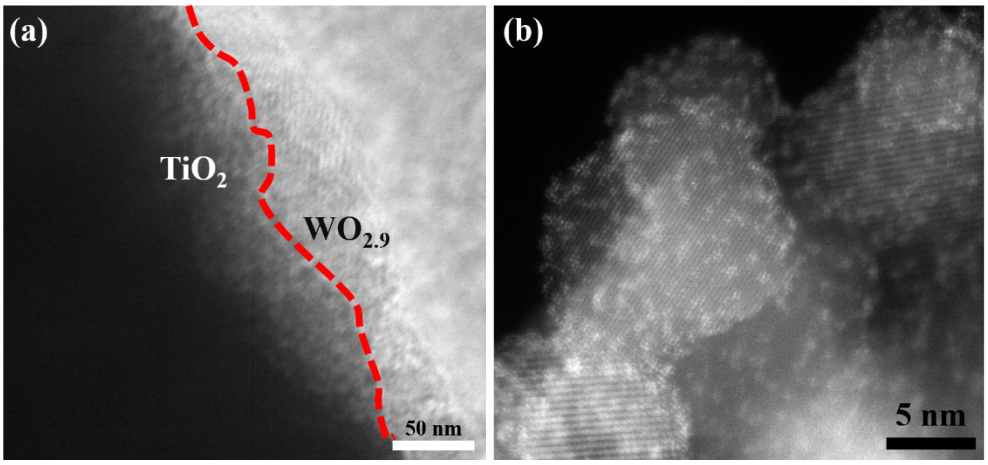

Figure S6. (a) High resolution TEM image at the edge of the sample Pt-$WO_{2.9}$/TiO_2 microspheres; (b) Aberration-corrected HAADF-STEM image of Pt-$WO_{2.9}$/TiO_2.

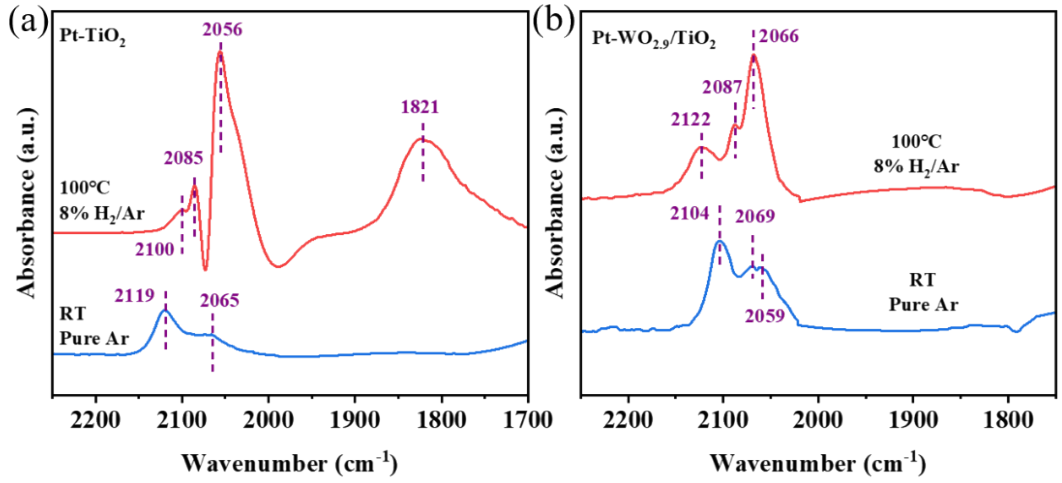

Figure S7. CO-DRIFTS spectra of (a) Pt- TiO_2 and (b) Pt-$WO_{2.9}$/TiO_2 after treatment in H_2/Ar.

Noticeably, a new band at 1821 cm^{-1} is evolved on Pt-TiO_2 after pretreatment (**Fig. S7a**), which is attributed to bridge-adsorbed CO on neighboring Pt atoms over the Pt NPs.[1] Such band is not observed for Pt-$WO_{2.9}$/TiO_2 (**Fig. S7b**), indicating that Pt atoms on $WO_{2.9}$ are strongly bond and highly dispersed. For both samples, the relative intensity of CO peaks ranging from 2050 to 2070 cm^{-1} increases, and the peak in the range from 2080 to 2120 cm^{-1} decrease, indicating that heating in reducing atmosphere leads to the partial reduction of $Pt^{\delta+}$ to Pt^0 and aggregation, but the phenomena is less dominate for Pt-$WO_{2.9}$/TiO_2.

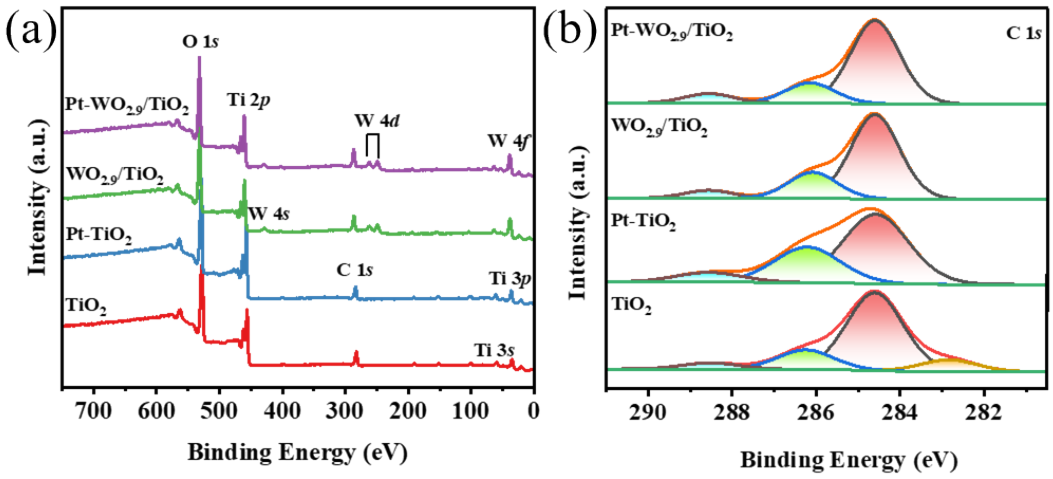

Figure S8. (a) XPS survey spectra and (b) C 1*s* of TiO_2, $WO_{2.9}/TiO_2$ and Pt-$WO_{2.9}/TiO_2$. The XPS spectra of Pt-TiO_2 is analyzed for reference as well.

Table S2. Analysis on the elemental composition obtained from XPS fitting results.

Samples	Percentage (%)				
	W^{5+}	W^{6+}	Pt^{0}	Pt^{2+}	Pt^{4+}
Pt-TiO_2	-	-	22.6	55.3	22.1
$WO_{2.9}$-TiO_2	13.7	86.3	-	-	-
Pt-$WO_{2.9}/TiO_2$	13.0	87.0	15.7	55.0	29.3

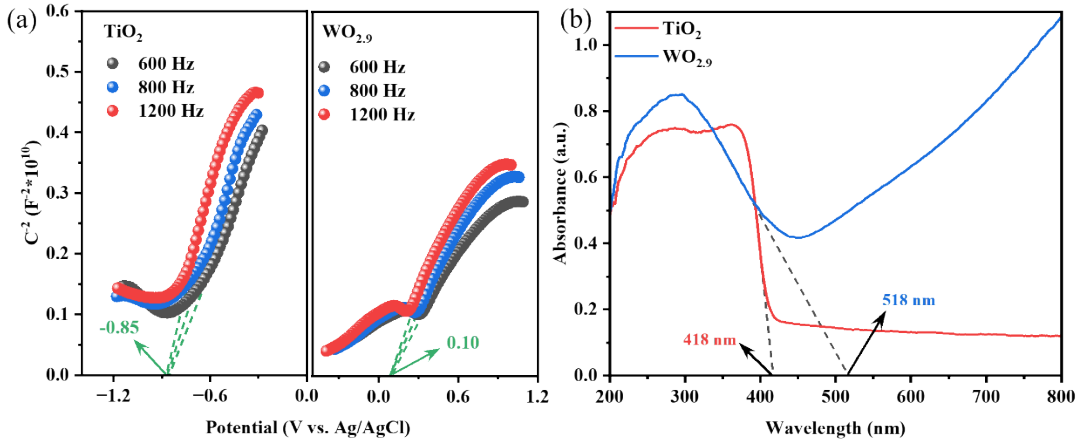

Figure S9. (a) The Mott-Schottky spectra of TiO_2 and $WO_{2.9}$; (b) UV–vis absorption spectra of TiO_2 and $WO_{2.9}$.

The UV-vis diffuse reflectance spectrum of TiO_2 shows absorption range of TiO_2 is $\lambda<418$ nm. Absorption of $WO_{2.9}$ is extended to $\lambda>400$ nm, that may be attributed to polaron transitions. Specifically, electrons trap at the W^{5+} sites interact with the lattice to form polarons, which result in the hopping of polarons from W^{5+} to nearby W^{6+} positions, that eventually cause visible or near infrared light absorption.

Table S3. Comparison on the activity and selectivity for photocatalytic CO_2 reduction in this work.

Photocatalysts	Average production rate (μmol g^{-1} h^{-1})			S_{CH4}	S_{CO2}
	H_2	CH_4	CO		
TiO_2	0.56	0.27	0.06	94.9%	67.1%
Pt-TiO_2	6.85	6.27	0.08	99.7%	78.6%
$WO_{2.9}$/TiO_2	0.13	0.61	0.10	96.2%	95.0%
Pt-$WO_{2.9}$/TiO_2	1.42	10.74	0.10	99.8%	96.8%
Pt NPs-$WO_{2.9}$/TiO_2	19.19	5.25	0.02	99.9%	52.4%

Table S4. Comparison on the methane production rate and selectivity in this work to literature reports.

Catalyst	Reaction conditions	CH_4 production ($\mu mol\ g^{-1}\ h^{-1}$)	S_{CH_4}	S_{CO_2}	Ref.
Pt-$WO_{2.9}$/TiO_2	AM1.5 100 mW cm^{-2} CO_2 (g) and water vapor	10.74	99.8%	96.8%	This work
0.8% Pd-WO_{3-y}/TiO_{2-x}	Xe lamp 100 mW cm^{-2} CO_2 (g) and water vapor	3.34	100%	-	[2]
0.5% Pt-WO_3	500 W Xe lamp CO_2 (g) and water vapor	0.73	-	100%	[3]
3% Mo-$WO_3 \cdot 0.33H_2O$	500 W Xe lamp CO_2 (g) and water vapor	5.3	61.2%	-	[4]
Cu-TiO_2/WO_3	Xe lamp 300 mW cm^{-2} CO_2 (g) and water vapor	98.69	88.5%	-	[5]
(Pt/TiO_2)@rGO-2	320-780 nm 80 mW cm^{-2} CO_2 (g) and water vapor	41.3	99.1%	96.7%	[6]
V_O-Nb_2O_5 nanosheet	AM1.5 100 mW cm^{-2} CO_2 (g) and water vapor	19.14	94.1%	-	[7]
(730) facet PtCu/g-C_3N_4	300 W Xe lamp CO_2 (g) and water vapor	7.47	90.6%		[8]
PdCu/g-C_3N_4	300 W Xe lamp CO_2 (g) and water vapor	1.2	100%	-	[9]
Au-mesoporous TiO_2	300 W Xe lamp, IR lamp CO_2 (g) and water vapor	10.07	85.72%		[10]
TiO_2/MXene Ti_3C_2	300 W Xe lamp in situ generate CO_2 and water vapor ($NaHCO_3$ + HCl solution)	4.4	-	-	[11]

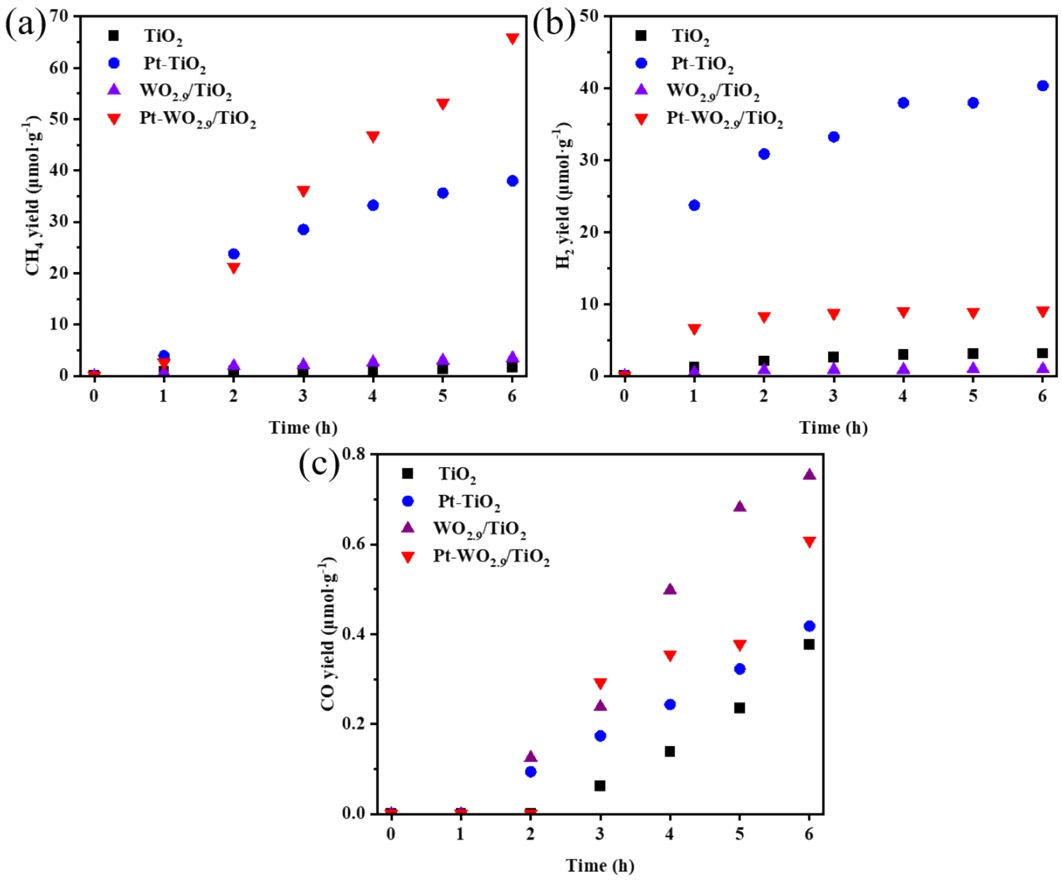

Figure S10. The comparison of CH_4 (a), H_2 (b), CO (c) yield over reaction time under illumination.

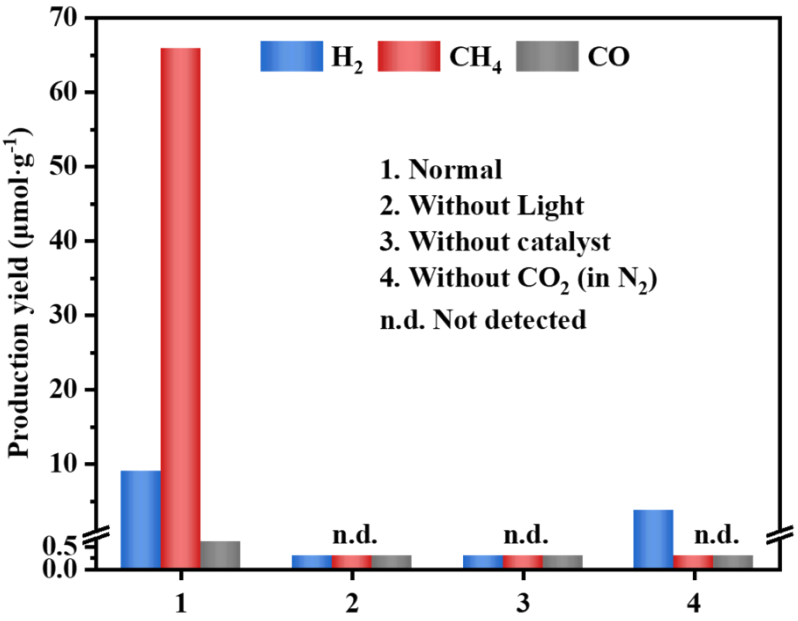

Figure S11. Photocatalytic CO_2 reduction activity for Pt-$WO_{2.9}$/TiO_2 under different experimental conditions.

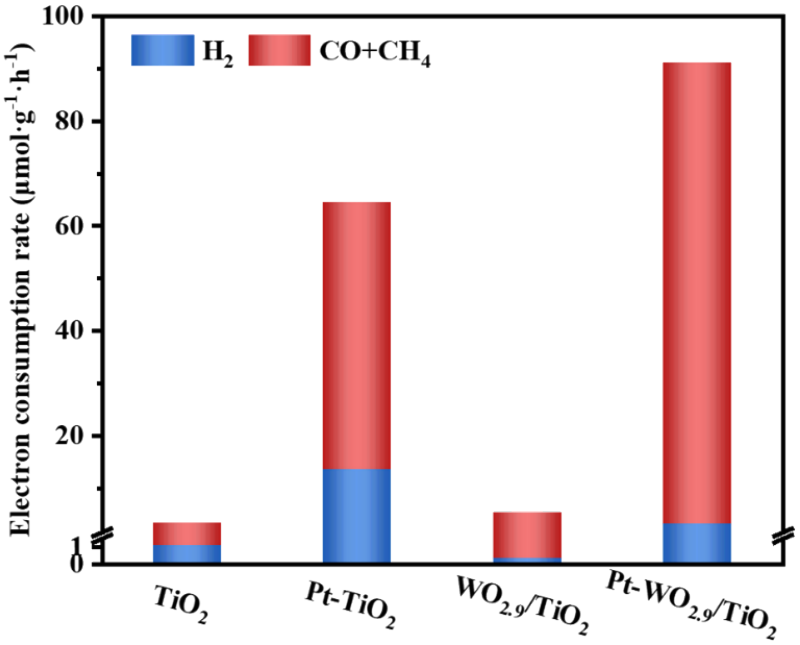

Figure S12. Electron consumption rate during CO_2 reduction of different samples.

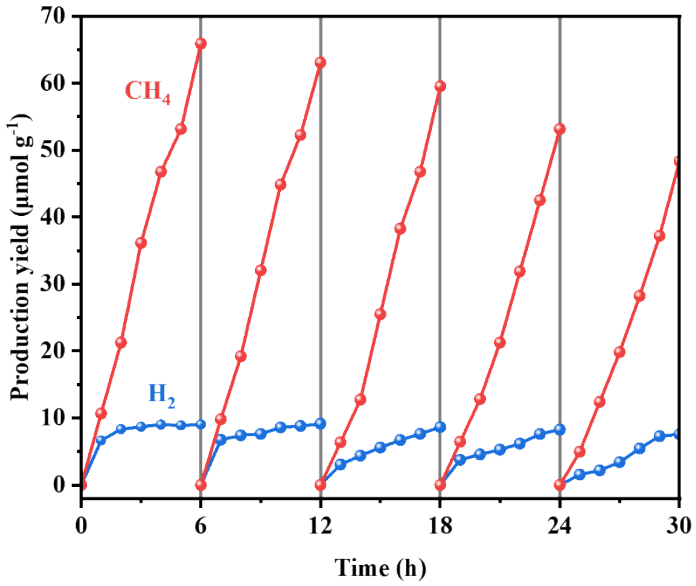

Figure S13. Cycling measurements for photocatalytic CO_2 reduction to CH_4 of Pt-$WO_{2.9}/TiO_2$

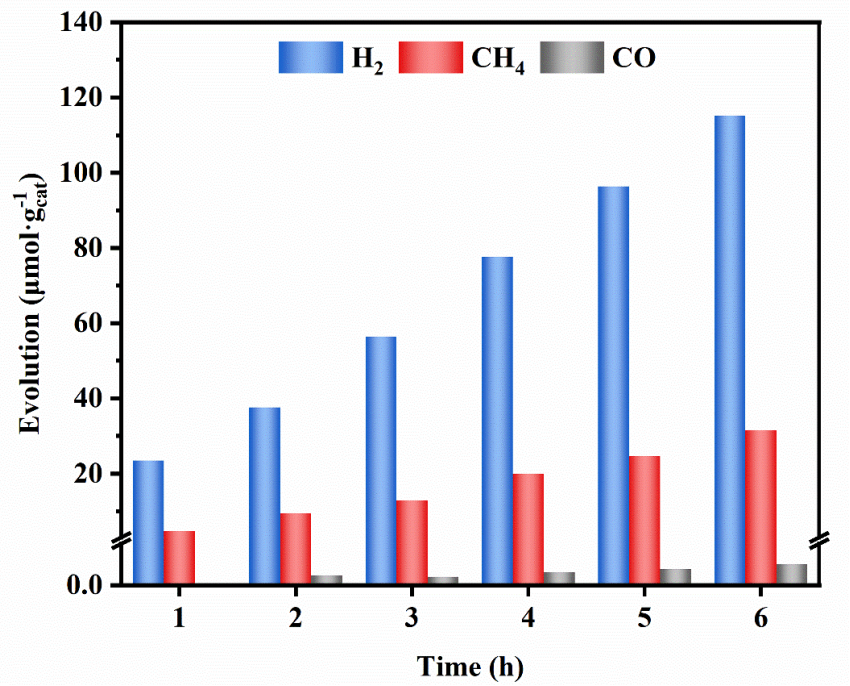

Figure S14. The evolution of H_2, CH_4 and CO over reaction time under illumination using Pt NPs on $WO_{2.9}/TiO_2$ in comparison to the samples with Pt_x on $WO_{2.9}/TiO_2$.

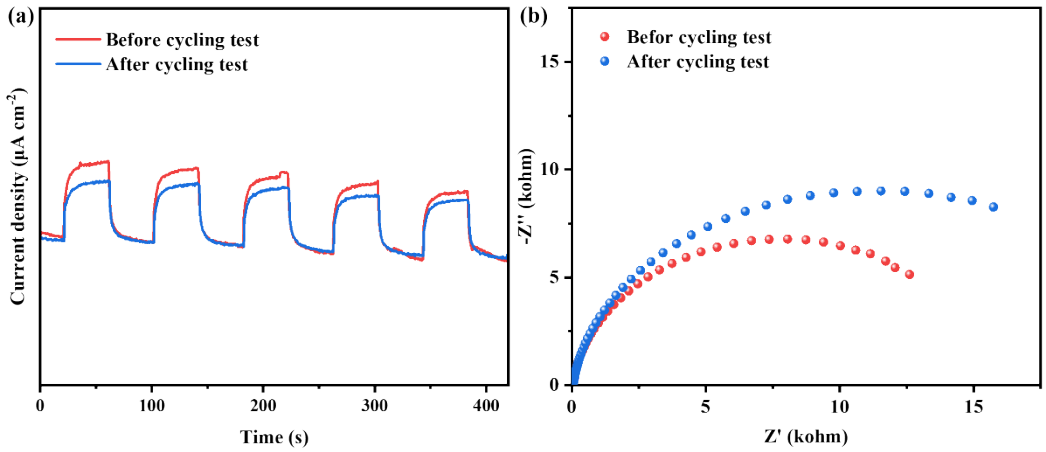

Figure S15. (a) Photocurrent transient spectra and (b) electrochemical impedance spectra (EIS) of Pt-$WO_{2.9}/TiO_2$ before and after photocatalytic stability tests.

Table S5. Parameters for EIS fitting. R_s: electrolyte resistance; R_{ct}: charge transfer resistance; Y_0, N, are parameters associated with the CPE; χ^2: fitting residues.

Photocatalysts	R_s/Ω	R_{ct}/KΩ	CPE		χ^2
			$\mathbf{Y_0}\times10^{-5}$	**N**	
TiO_2	13.82	131.91	2.15	0.90	0.0082
Pt-TiO_2	12.70	27.92	2.24	0.89	0.0050
$WO_{2.9}/TiO_2$	11.22	98.75	2.46	0.90	0.0107
Pt-$WO_{2.9}/TiO_2$	48.40	15.31	2.27	0.92	0.0160

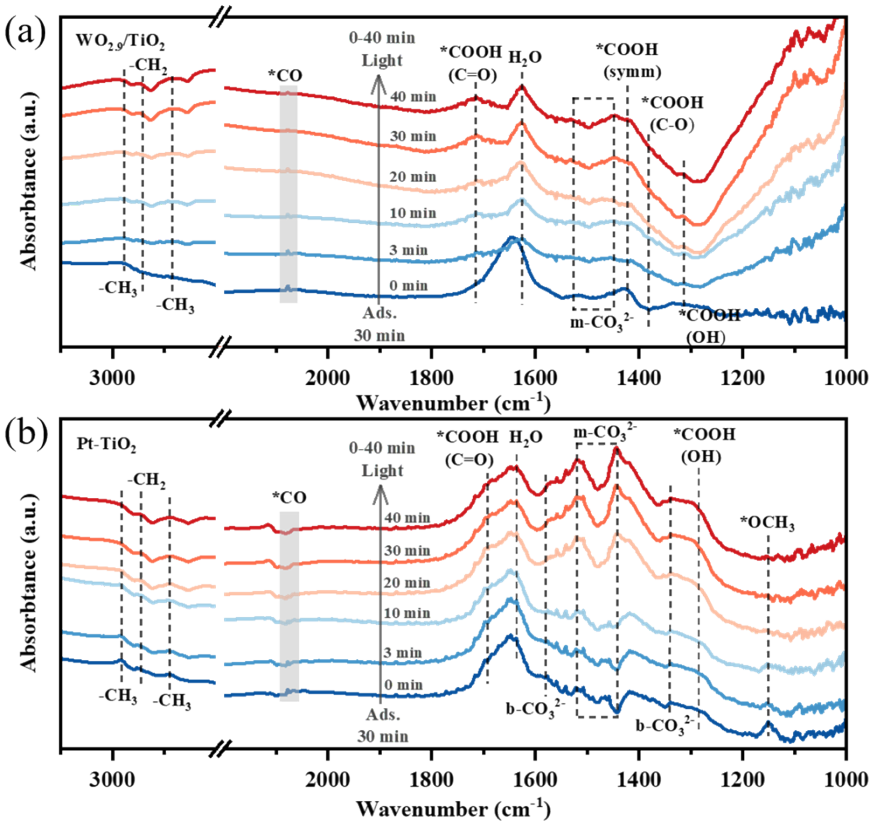

Figure S16. *In situ* DRIFTS spectra taken during photocatalytic CO_2 reduction using (a) $WO_{2.9}/TiO_2$ and (b) Pt-TiO_2.

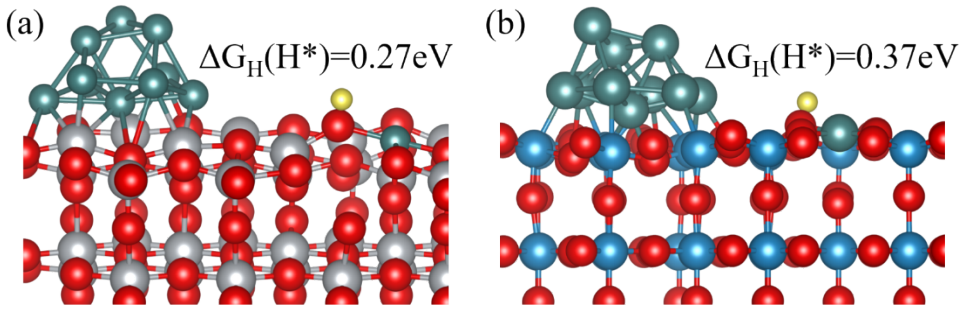

Figure S17. Stick-ball models of hydrogen adsorption on oxygen atoms adjacent to Pt_1 and the corresponding free energy: (a) Pt-TiO_2; (b) Pt-$WO_{2.9}$.

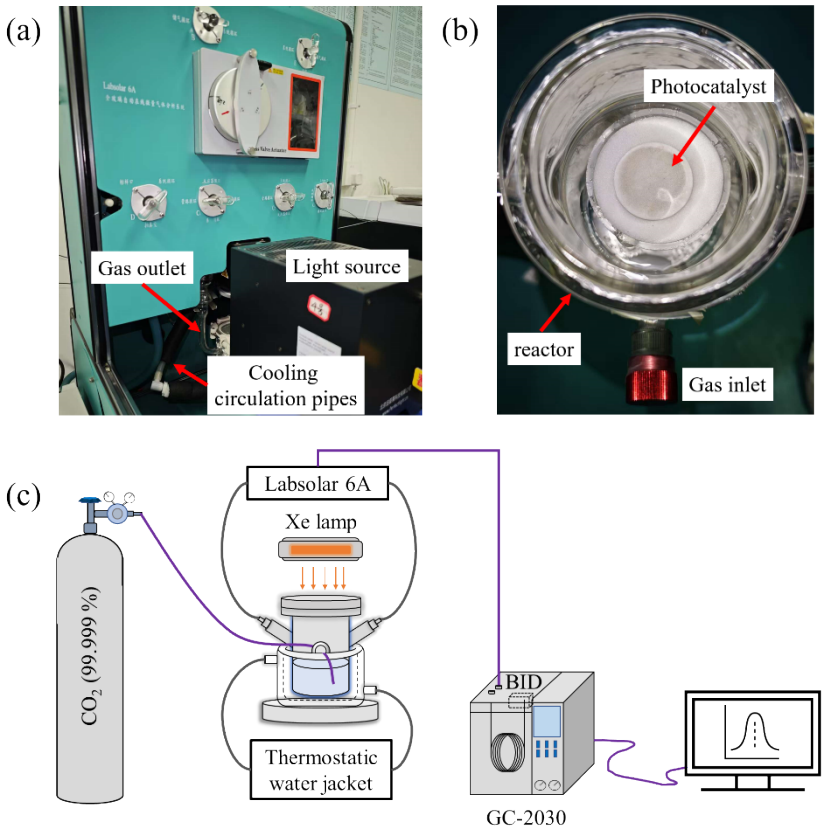

Figure S18. Photographs of (a) the photocatalytic system and (b) top view of the reactor; (c) simplified illustration of the photocatalytic system.

References:

1. W. Zhang, H. Wang, J. Jiang, Z. Sui, Y. Zhu, D. Chen and X. Zhou, *ACS Catalysis*, 2020, **10**, 12932-12942.
2. L. Shen, Z. Xie, L. Hou, J. Yang and Q. Li, *Energy & Fuels*, 2022, **36**, 11515-11523.
3. H. Wang, L. Zhang, Y. Zhou, S. Qiao, X. Liu and W. Wang, *Applied Catalysis B: Environmental*, 2020, **263**, 118331.
4. H. Wang, L. Zhang, K. Wang, X. Sun and W. Wang, *Applied Catalysis B: Environmental*, 2019, **243**, 771-779.
5. H. Zhang, Q. Liu and Z. Shen, *Chin. Chem. Lett.*, 2024, **35**, 108607.
6. Y. Zhao, Y. Wei, X. Wu, H. Zheng, Z. Zhao, J. Liu and J. Li, *Applied Catalysis B: Environmental*, 2018, **226**, 360-372.
7. J. Wu, J. Zhu, W. Fan, D. He, Q. Hu, S. Zhu, W. Yan, J. Hu, J. Zhu, Q. Chen, X. Jiao and Y. Xie, *Nano Lett.*, 2024, **24**, 696-702.
8. Q. Lang, Y. Yang, Y. Zhu, W. Hu, W. Jiang, S. Zhong, P. Gong, B. Teng, L. Zhao and S. Bai, *Journal of Materials Chemistry A*, 2017, **5**, 6686-6694.
9. L. Zhao, F. Ye, D. Wang, X. Cai, C. Meng, H. Xie, J. Zhang and S. Bai, *ChemSusChem*, 2018, **11**, 3524-3533.
10. S. Cai, J. Chen, Q. Li and H. Jia, *ACS Applied Materials & Interfaces*, 2021, **13**, 14221-14229.
11. J. Low, L. Zhang, T. Tong, B. Shen and J. Yu, *J. Catal.*, 2018, **361**, 255-266.